Selective coordination of three transition metal ions within a coiled-coil peptide scaffold

SUPPORTING INFORMATION

Aimee L. Boyle,[a]* Martin Rabe,[b] Niek S. A. Crone,[a] Guto G. Rhys,[c] Nicolas Soler,[d] Patrick Voskamp,[a] Navraj S. Pannu,[a] and Alexander Kros[a]

[a] Leiden Institute of Chemistry, Gorlaeus Laboratories, Leiden University, Einsteinweg 55, 2333 CC Leiden, The Netherlands

[b] Max-Planck-Institut für Eisenforschung GmbH, Max-Planck-Straße 1, 40237 Düsseldorf, Germany

[c] School of Chemistry, University of Bristol, Cantock's Close, Bristol, BS8 1TS, United Kingdom

[d] Structural Biology Unit, Institute of Molecular Biology of Barcelona (IBMB-CSIC), Baldiri Reixac 15, 08028 Barcelona, Spain

* Corresponding author. Email: a.l.boyle@chem.leidenuniv.nl

Contents:

CD spectra of HisA and HisD
Full NMR spectra of HisAD, HisAD-Cu(II), and HisAD-Ni(II)
NMR spectra of CC-Tri and HisAD-WY in the absence and presence of Cu(II)
AUC data of the HisAD-Cu(II) and HisAD-Ni(II) complexes
Comparisons of crystal structures of CC-Tri and HisAD
Bond lengths and angles for Cu(II)-ligand interactions in HisAD-Cu(II)
Thermal melts of HisAD:Cu and HisAD:Ni complexes
CD Titrations of HisAD with Zn(II) and Co(II)
222 nm plots of titration data used to determine dissociation constants for HisAD:Cu and HisAD:Ni complexes
Fits of CD titration data to a two-state model
Detailed discussion of methods and equations used to determine dissociation constants
Fitting parameters from the three-state model with a P_3M_1 intermediate
Data and fits for alternative intermediates for the three-state fitting model
LCMS spectra for HisA, HisD, HisAD, CC-Tri and HisAD-WY

CD spectra of HisA and HisD

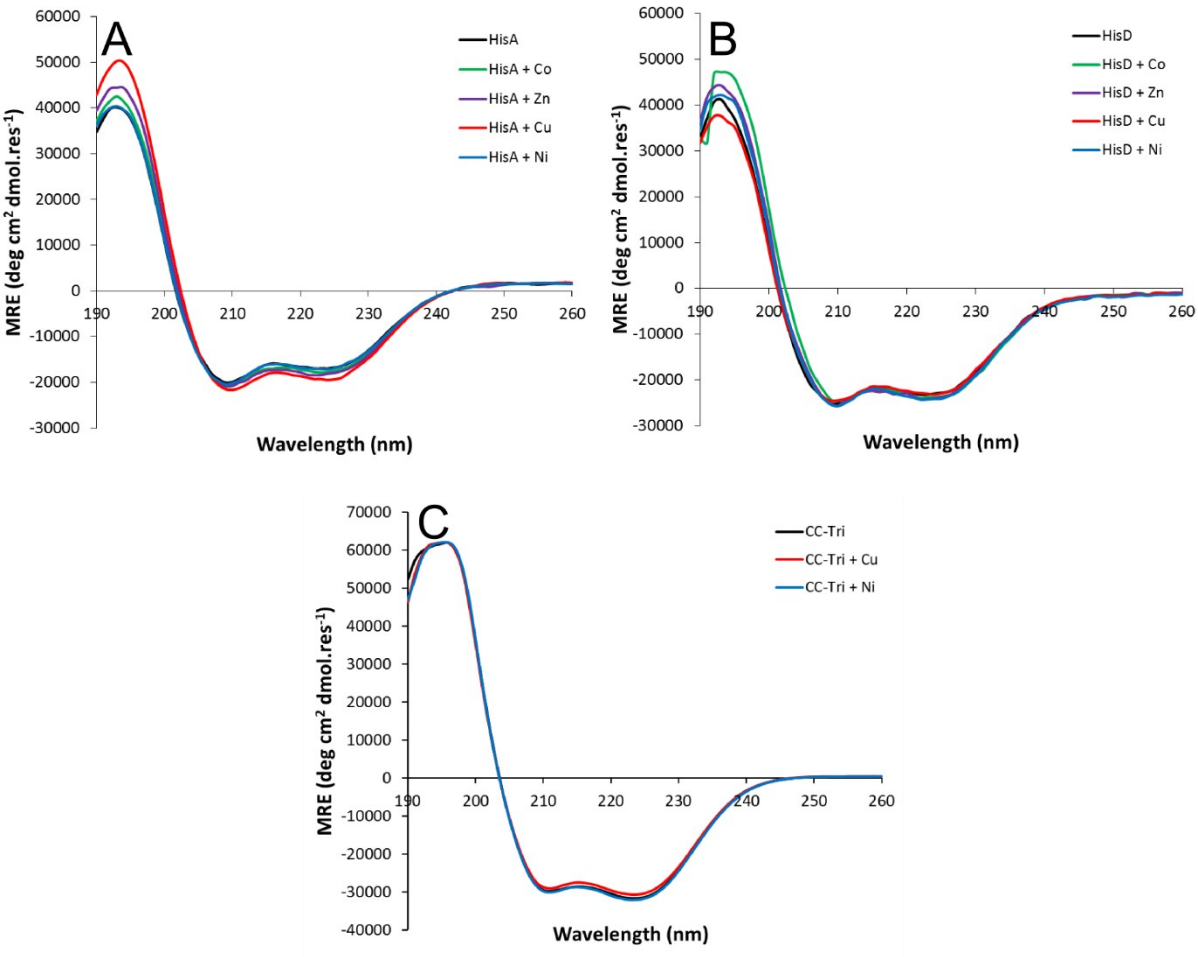

Figure S1. CD spectra of (A) HisA, (B) HisD and (C) CC-Tri in the absence and presence of metals. Conditions: [peptide] = 100 µM, (where appropriate) [metal] = 100 µM, 10 mM phosphate buffer, pH 7.4, 20 °C.

Full NMR spectra of HisAD, HisAD-Cu(II), and HisAD-Ni(II)

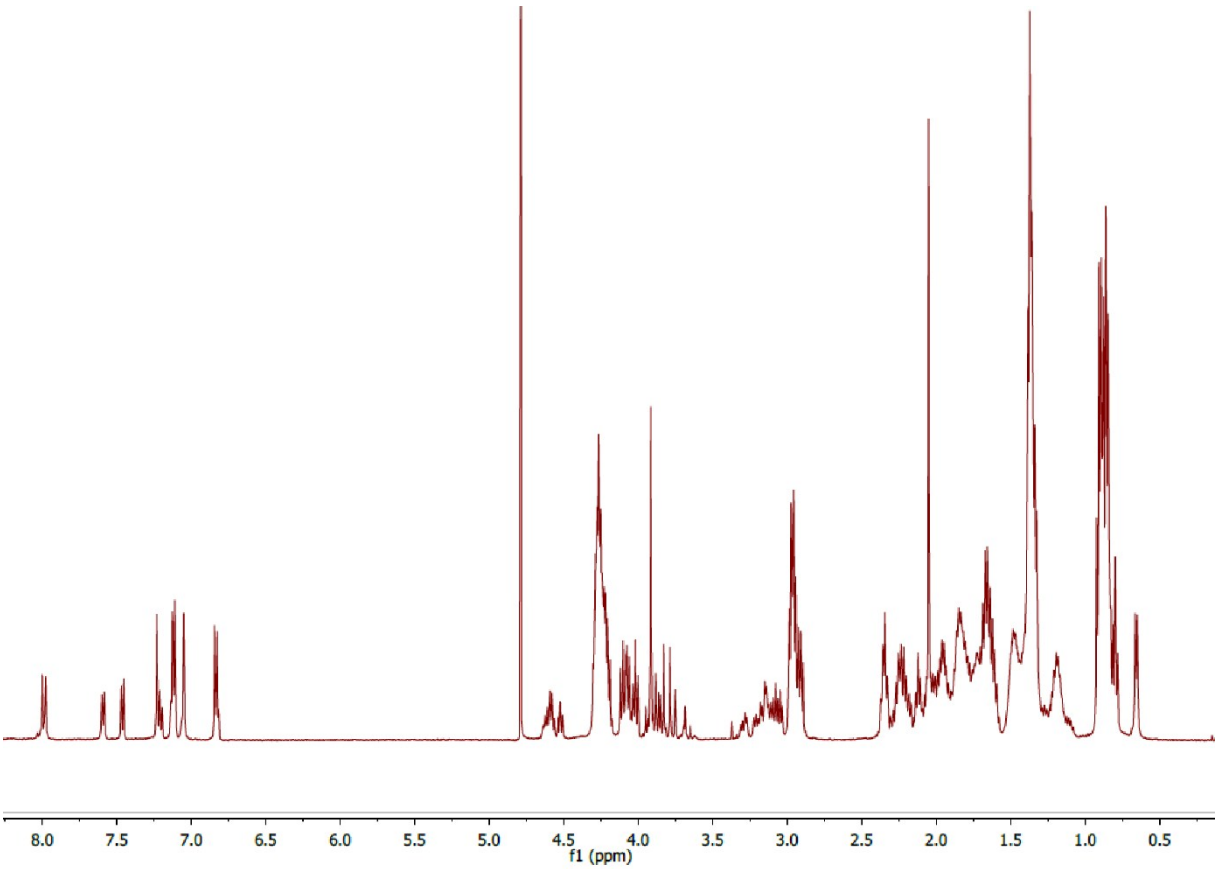

Figure S2. Complete ^{1}H NMR spectrum of HisAD.
Conditions: [peptide] = 500 µM, 10 mM deuterated phosphate buffer, pH 7.4.

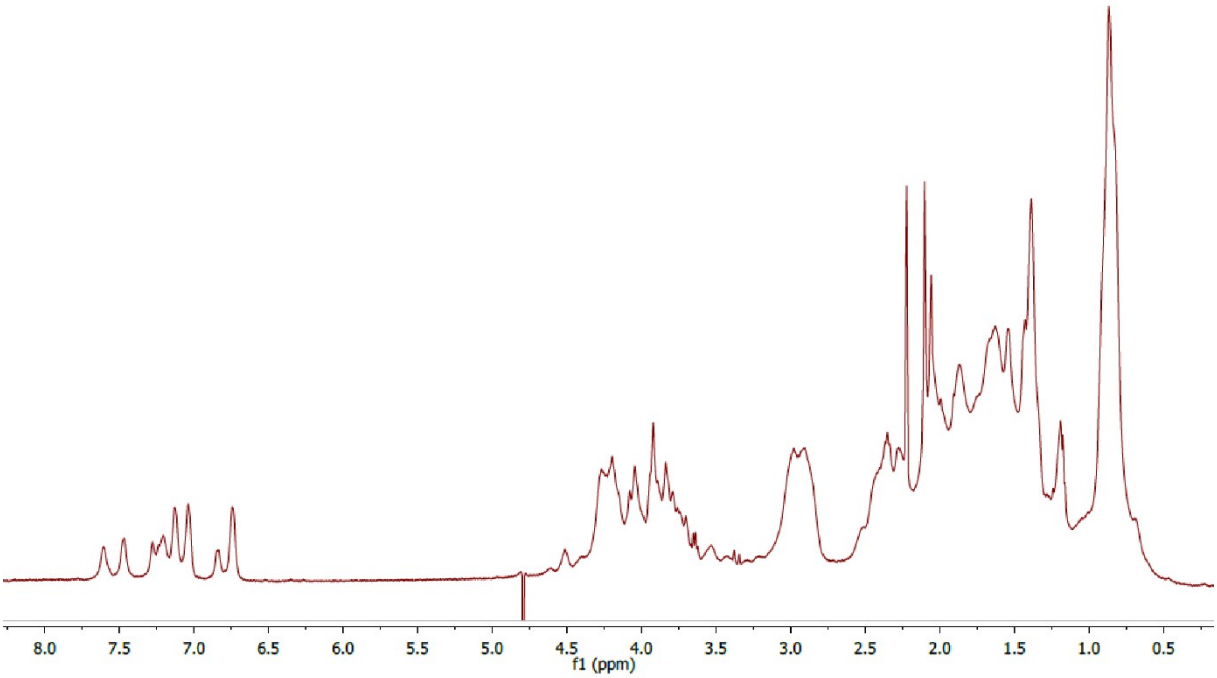

Figure S3. Complete ^{1}H NMR spectrum of HisAD with 1 equivalent of Cu(II).
Conditions: [peptide] = 500 µM, [Cu(II)] = 500 µM, 10 mM deuterated phosphate buffer, pH 7.4.

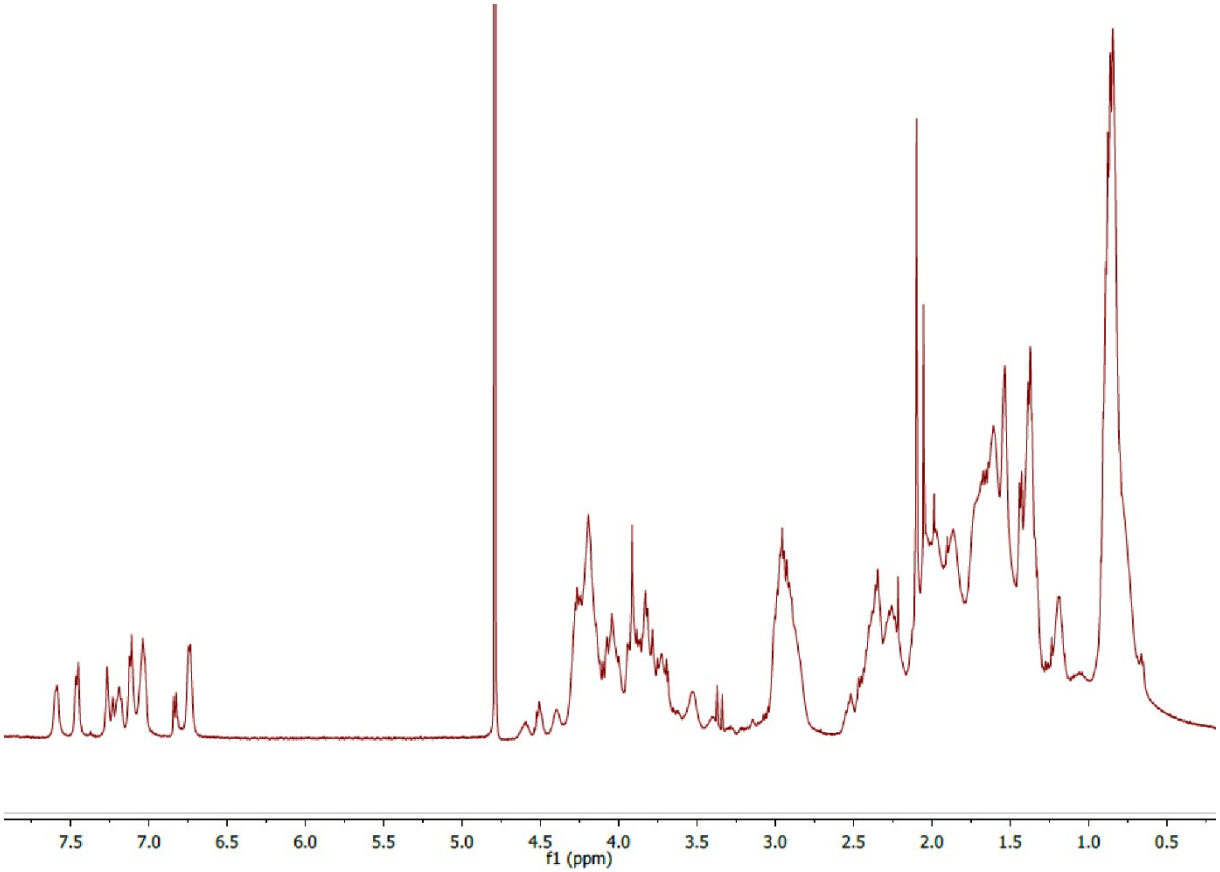

Figure S4. Complete ^{1}H NMR spectrum of HisAD with 1 equivalent of Ni(II).
Conditions: [peptide] = 500 μM, [Ni(II)] = 500 μM, 10 mM deuterated phosphate buffer, pH 7.4.

NMR Spectra for CC-Tri, and HisAD-WY

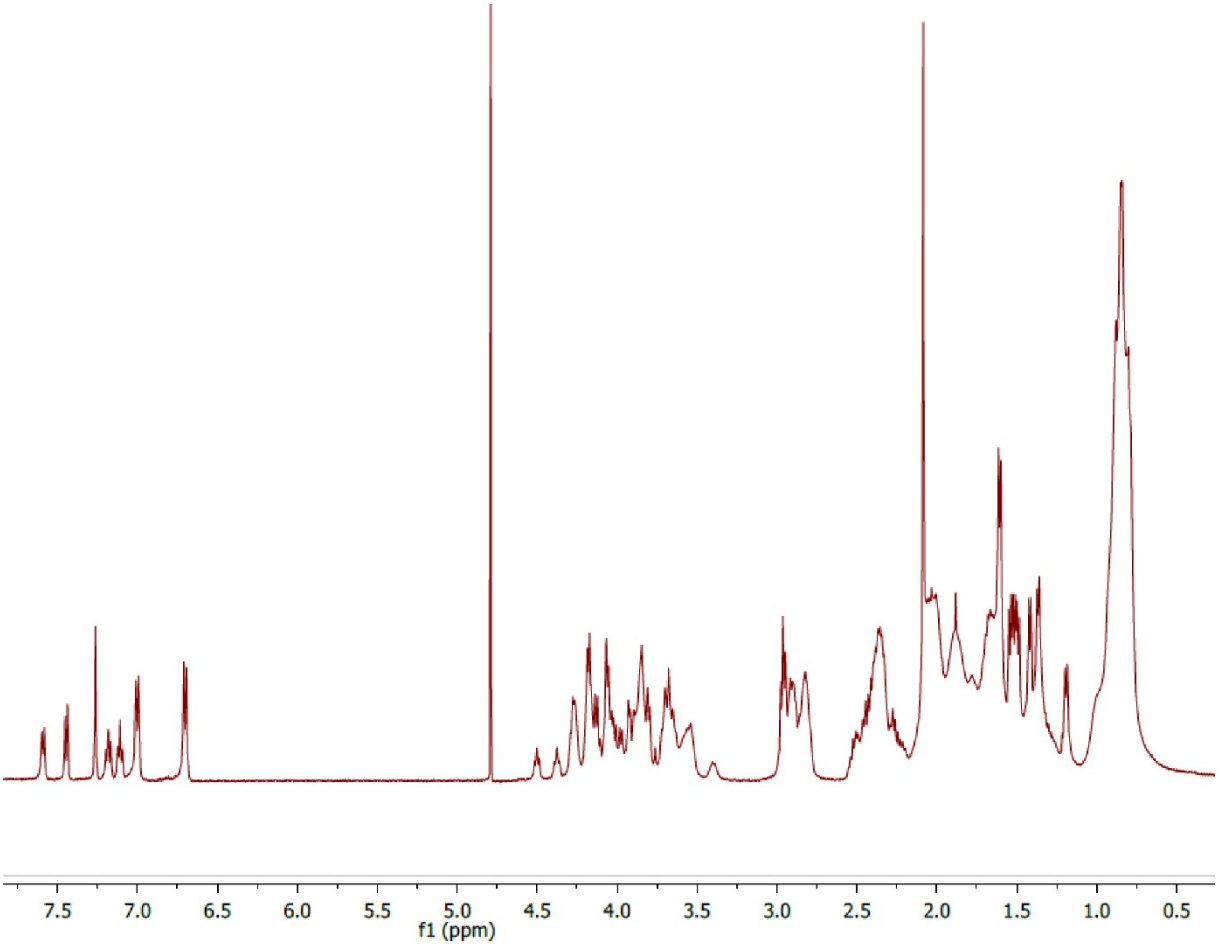

Figure S5. Complete ^{1}H NMR spectrum for CC-Tri.
Conditions: [peptide] = 500 μM, 10 mM deuterated phosphate buffer, pH 7.4.

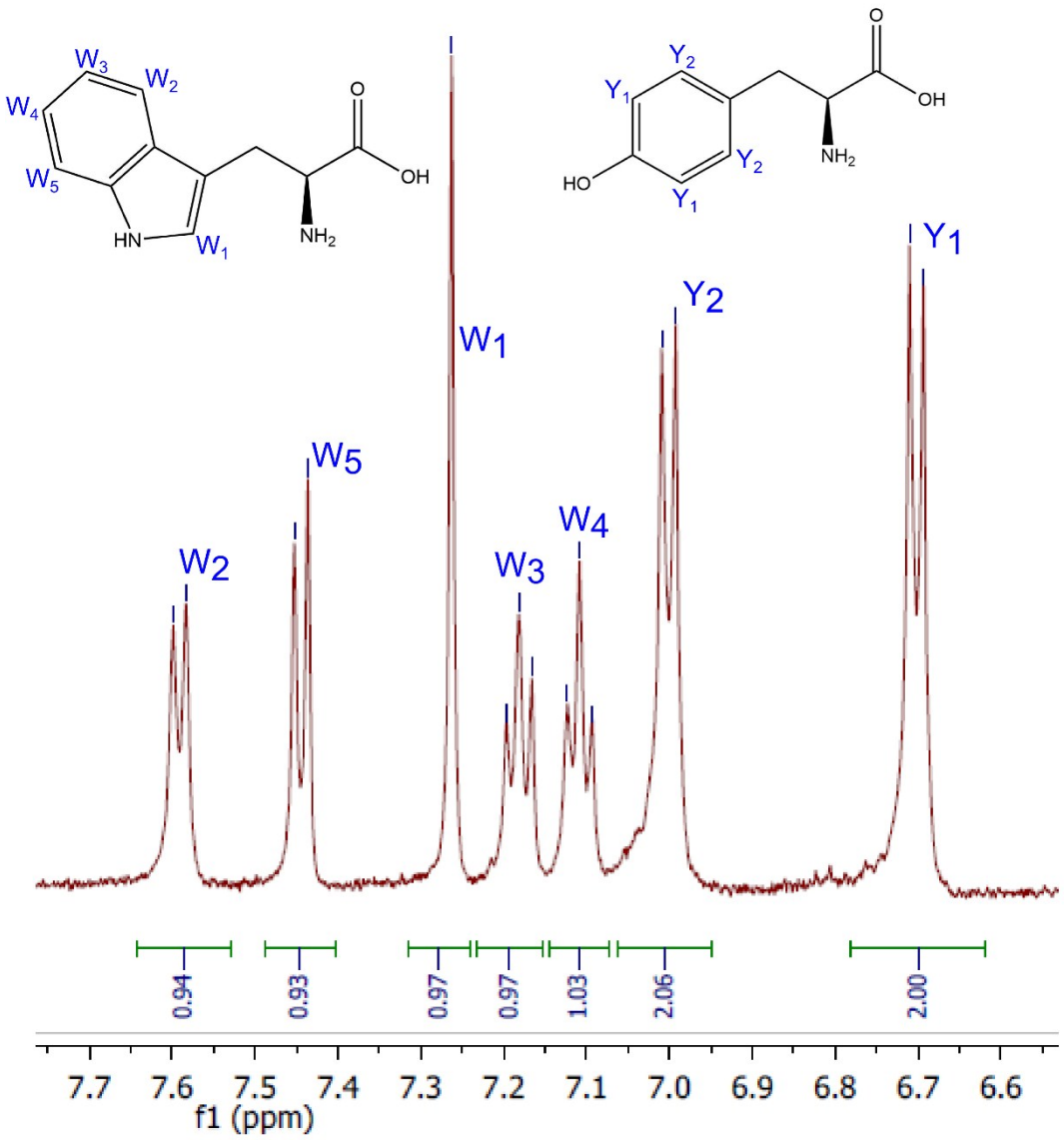

Figure S6. ^{1}H NMR spectrum of the aromatic region of CC-Tri. The resonances have been assigned to their specific protons.
Conditions: [peptide] = 500 µM, 10 mM deuterated phosphate buffer, pH 7.4.

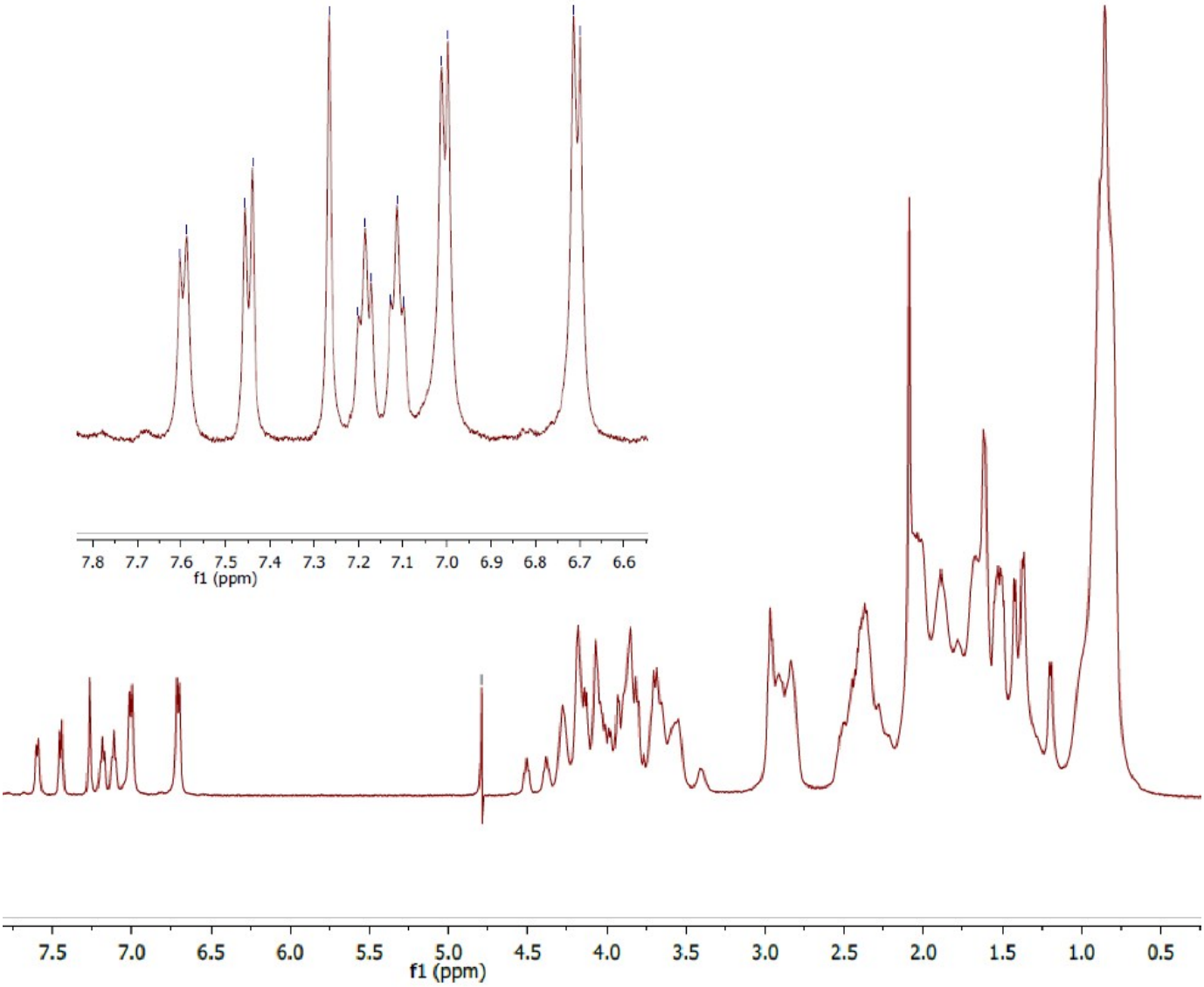

Figure S7. ^{1}H NMR spectrum of CC-Tri with 1 equivalent of Cu(II), the inset shows the aromatic region in more detail and this is no different to the spectrum collected in the absence of Cu(II), indicating Cu(II) does not perturb the folding of CC-Tri.
Conditions: [peptide] = 500 μM, [Cu(II)] = 500 μM, 10 mM deuterated phosphate buffer, pH 7.4.

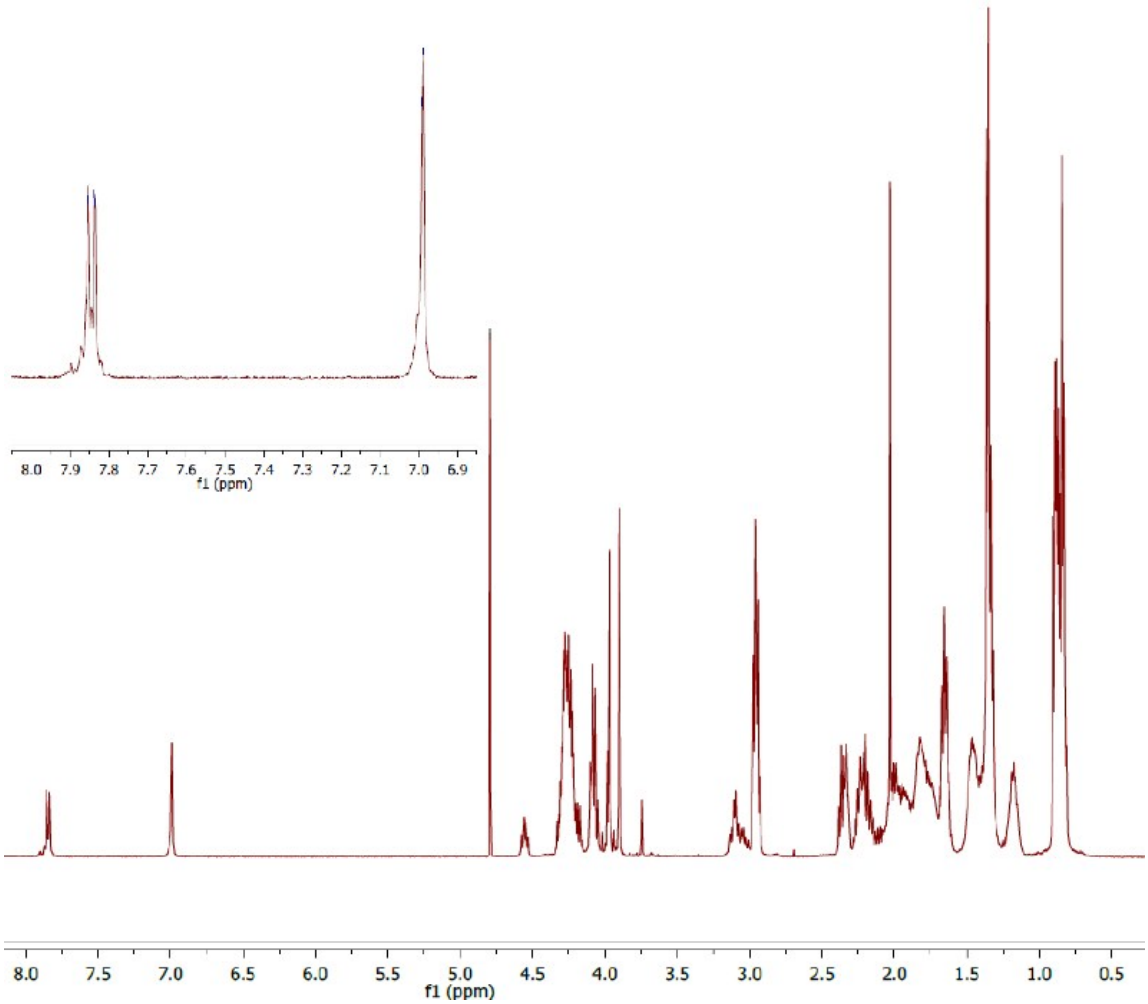

Figure S8. ^{1}H NMR spectrum of HisAD-WY (HisAD with the Trp and the Tyr residues substituted for Gln and Gly respectively). The inset shows a close-up of the aromatic region, with the resonances of the histidine protons evident.
Conditions: [peptide] = 500 µM, 10 mM deuterated phosphate buffer, pH 7.4.

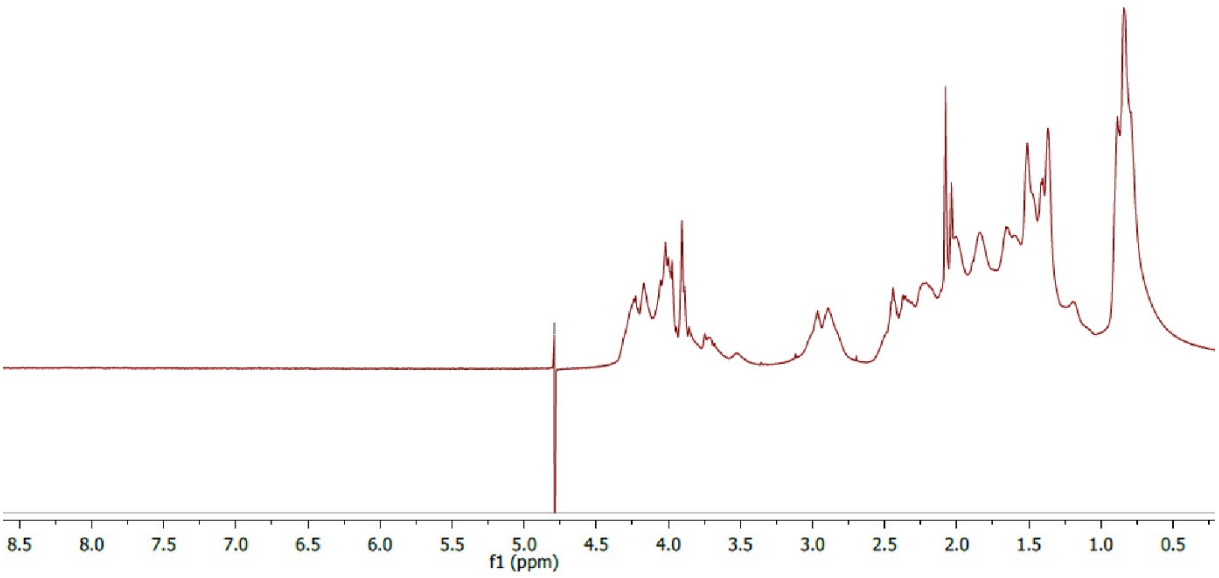

Figure S9. ^{1}H NMR spectrum of HisAD-WY with Cu(II). The resonances from the histidines are absent.
Conditions: [peptide] = 500 µM, [Cu(II)] = 500 µM, 10 mM deuterated phosphate buffer, pH 7.4.

AUC data of the HisAD-Cu(II) and HisAD-Ni(II) complexes

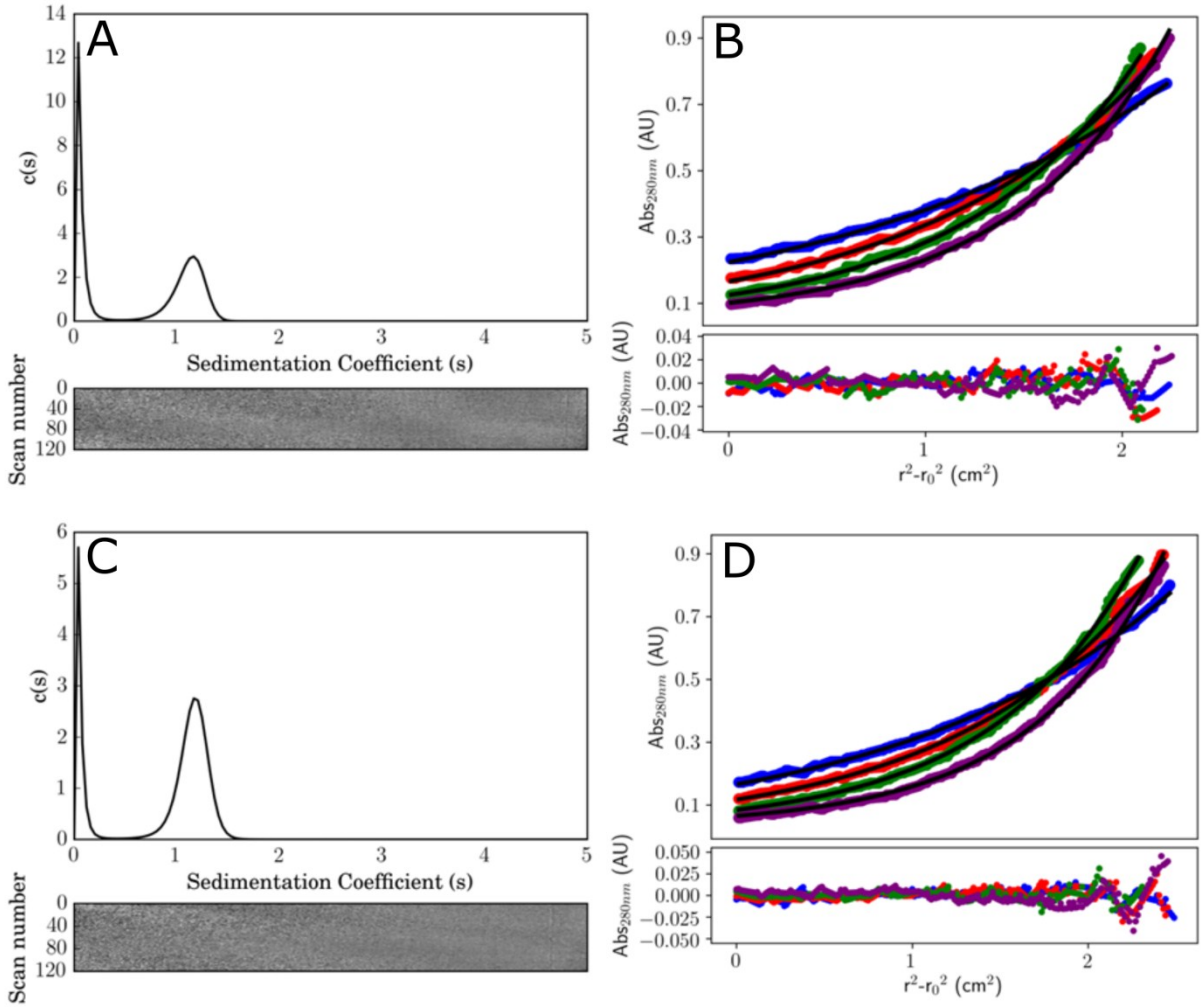

Figure S10. AUC data for HisAD-Cu(II) and HisAD-Ni(II). (A) Sedimentation-velocity continuous c(s) distribution for HisAD-Cu(II). The experiment was conducted at 60k rpm returning a best-fit f/f_0 = 1.247, s = 1.110 S, $s_{20,w}$ = 1.273 S and Mw = 9,399 Da (2.7 x monomer mass) at 95% confidence level. Residuals are shown as a bitmap, (lower panel), in which the greyscale shade indicates the difference between the fitted and raw data, scans are ordered vertically. The horizontal axis is the radial range over which the data were fitted.
(B) Sedimentation-equilibrium data (dots in upper panel) and fitted single ideal species model curves (black lines) at 33k (blue), 39k (red), 45k (green) and 48k (purple) rpm. The fit returns a mass of 9,940 Da (2.8 monomer mass, 95% confidence interval 9,905–9,981 Da). The lower panel contains the residuals for the fits using the same colour scheme. (C) Sedimentation-velocity continuous c(s) distribution for HisAD-Ni(II). The experiment was conducted at 60k rpm returning a best-fit f/f_0 = 1.291, s = 1.158 S, $s_{20,w}$ = 1.293 S and mw = 10,121 Da (2.9 x monomer mass) at 95% confidence level. Residuals are shown as a bitmap (lower panel) in which the greyscale shade indicates the difference between the fitted and raw data, scans are ordered vertically. The horizontal axis is the radial range over which the data were fitted. (D) sedimentation-equilibrium data (dots in upper panel) and fitted single ideal species model curves (black lines) at 33k (blue), 39k (red), 45k (green) and 48k (purple) rpm. The fit returns a mass of 10,510 Da (3.0 monomer mass, 95% confidence interval 10,448–10,532 Da). The lower panel contains the residuals for the fits using the same colour scheme.
Conditions: [peptide] = 200 μM, [$NiCl_2$] = 1 mM, [$CuCl_2$] = 200 μM, PBS buffer: 100 mM NaCl, 8.02 mM K_2HPO_4, 1.98 mM KH_2PO_4, pH 7.4.

Comparisons of crystal structures of CC-Tri and HisAD

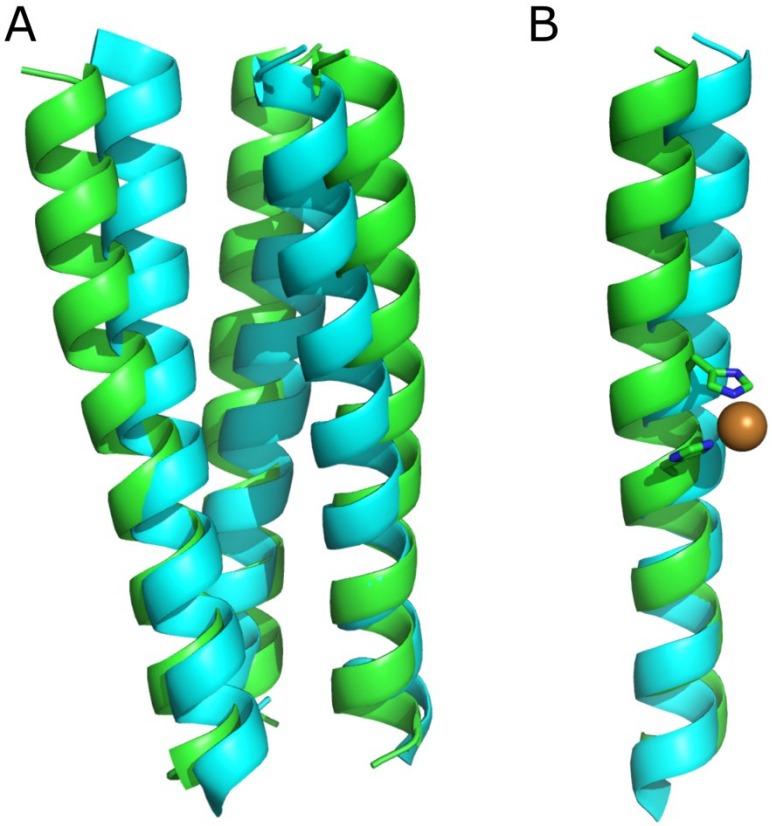

Figure S11. Overlay of CC-Tri (blue) and HisAD (green) showing (A) the deviation of the HisAD structure from the packing of the CC-Tri structure from the C-termini (bottom), to the N-termini (top). The radius at the N-terminus (Cα-Cα distances between Glu2 residues) of CC-Tri is 12.1 Å, whereas HisAD has a radius of 14.8 Å. (B) The histidine residues coordinating the Cu(II) ion, are drawn as sticks to highlight that it is the relative orientation of these residues to allow them to coordinate Cu(II) that causes the distortion of the helical packing.

Bond lengths and angles for Cu(II)-ligand interactions in HisAD-Cu(II)

Bond Length (Å)		**Bond Angle (°)**	
N(His13) – Cu	1.9	N(His13) – Cu – N(His17)	101.9
N(His17) – Cu	2.1	N(His13) – Cu – O1(Glu16)	148.3
O1(Glu16) – Cu	2.3	N(His13) – Cu – O2(Glu16)	151.4
O2(Glu16) – Cu	2.2	N(His13) – Cu – O(Glu2)	82.7
O(Glu2) – Cu	2.2	N(His17) – Cu – O1(Glu16)	81.8
		N(His17) – Cu – O2(Glu16)	89.3
		N(His17) – Cu – O(Glu2)	114.4
		O1(Glu16) – Cu – O(Glu2)	67.5
		O2(Glu16) – Cu – O(Glu2)	116.7
		O1(Glu16) – Cu – O2(Glu16)	58.7

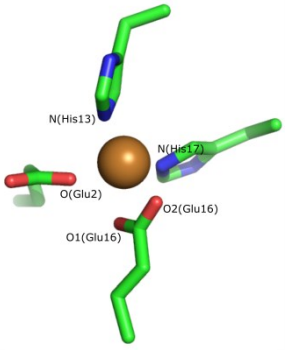

Table S1. Bond lengths and angles for all ligands coordinating the Cu(II) ion in the X-ray crystal structure of the HisAD-Cu(II) complex. The scheme on the right of the table identifies the coordinating atoms.

Thermal melts of HisAD:Cu and HisAD:Ni complexes

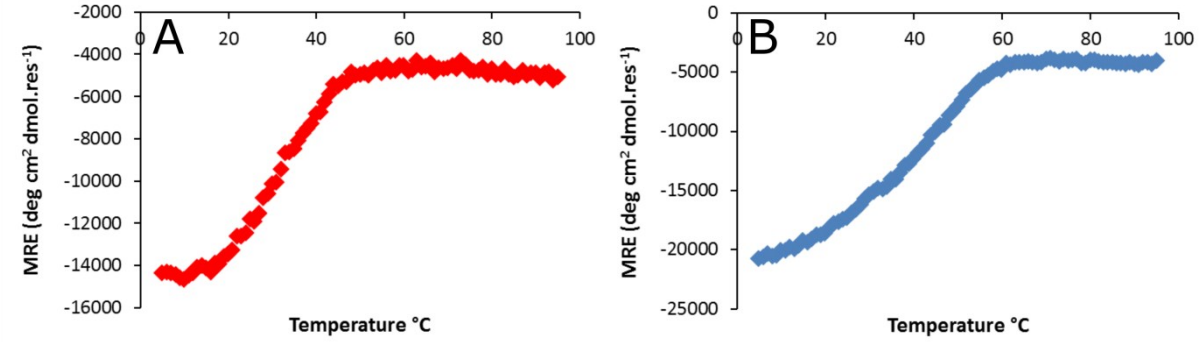

Figure S12. Thermal unfolding curves of HisAD with Cu(II) and Ni(II) monitored at 222 nm, from 5 – 95 °C, by CD spectroscopy. (A) Unfolding curve for the HisAD:Cu complex; (B) unfolding curve for the HisAD:Ni complex.
Conditions: [peptide] = 100 µM, [metal] = 100 µM, 10 mM phosphate buffer pH 7.4.

CD Titrations of HisAD with Zn(II) and Co(II)

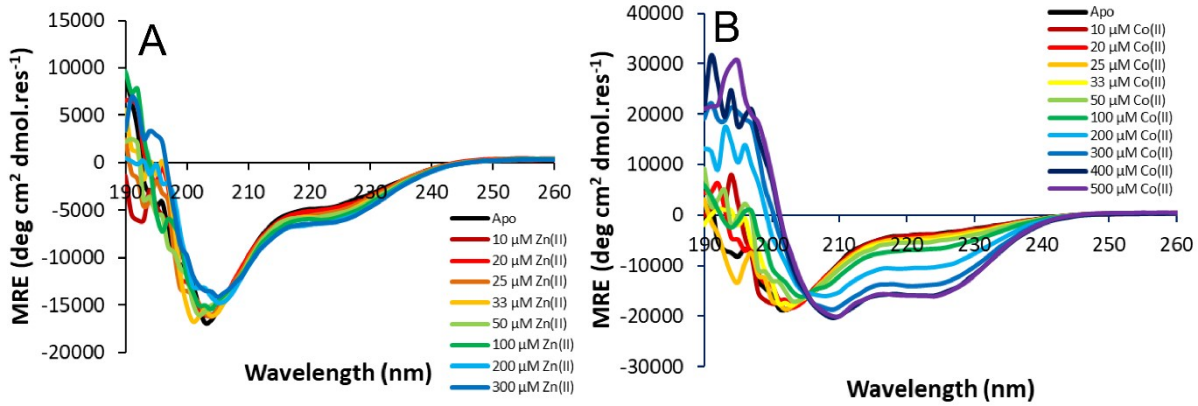

Figure S13. Titration curves monitored by CD for (A) Zn(II) and (B) Co(II). Conditions: [peptide] = 100 µM, 10 mM phosphate buffer, pH 7.4, 20 °C.

222 nm plots of data used to determine dissociation constants for HisAD-Cu(II) and HisAD-Ni(II) complexes

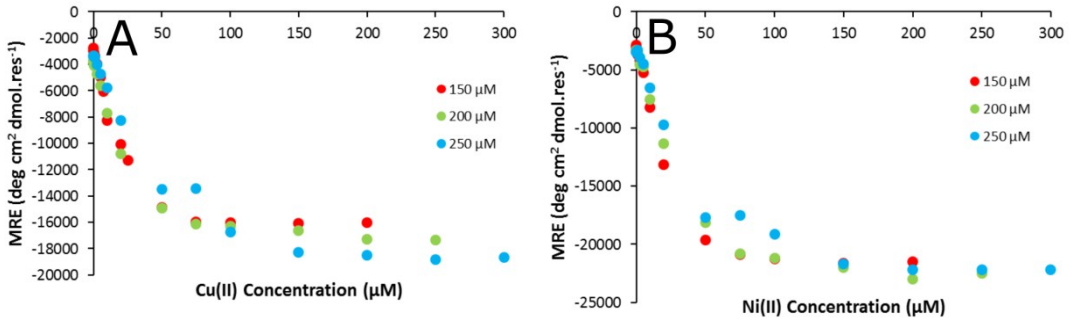

Figure S14. Titration curves monitored by CD spectroscopy at 222 nm for (A) HisAD-Cu(II) and (B) HisAD-Ni(II). Titrations were conducted at three different peptide concentrations, as noted in the legends.
Conditions: 10 mM phosphate buffer, pH 7.4, 20 °C.

Fits of CD titration data to a two-state model

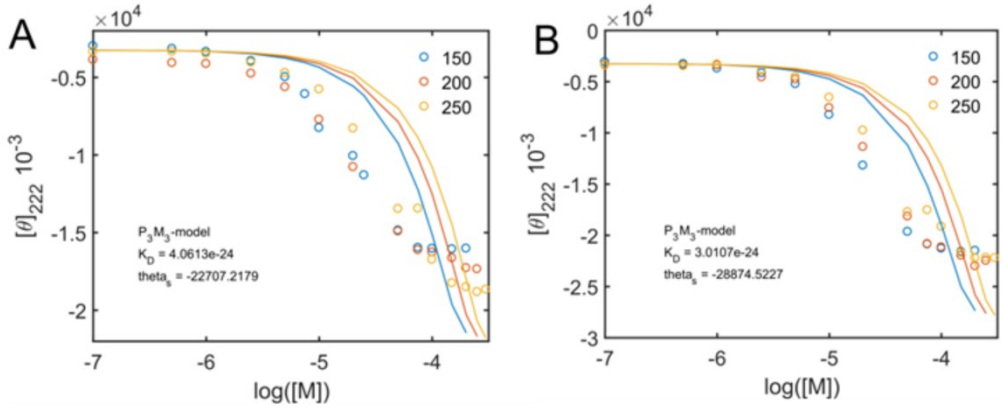

Figure S15. CD-titration data for the HisAD-Cu(II) complex at 150 µM peptide concentration, fitted to a two-state model of P_3M_3 dissociating into monomeric peptide chains and metal ions. This example shows that this model is not sufficient to describe the helicity measured at intermediate metal concentrations, therefore an additional intermediate state must be formed.

Detailed discussion of methods and equations used to determine dissociation constants

For fitting CD titration data to a 3-state folding model of a P_3M_3 complex via the intermediate $P_\rho M_\mu$, the anticipated dissociations are:

$$P_3M_3 \overset{K_{D3}}{\leftrightarrow} P_\rho M_\mu + (3-\rho)P + (3-\mu)M \overset{K_{Di}}{\leftrightarrow} 3P + 3M \tag{1}$$

For the dissociation constants K_{D3} , pK_{D3}, K_{Di} and pK_{Di} the equations 2 and 3 can be derived:

$$K_{Di} = 10^{-pK_{Di}} = \frac{[P]^\rho [M]^\mu}{[P_\rho M_\mu]} \tag{2}$$

$$K_{D3} = 10^{-pK_{D3}} = \frac{[P_\rho M_\mu][P]^{3-\rho}[M]^{3-\mu}}{[P_3M_3]} \tag{3}$$

with ρ and μ denoting the stoichiometric constants of the intermediate complex. The measured molar ellipticity at 222 nm ($[\theta]$) during the titration is:

$$[\theta] = \alpha_3[\theta]_{s3} + \alpha_i[\theta]_{si} + \beta[\theta]_f \tag{4}$$

$[\theta]_{s3}$ is the molar ellipticity of the fully saturated P_3M_3 complex, $[\theta]_{si}$ is the molar ellipticity of the intermediate complex and $[\theta]_f$ is the molar ellipticity of the free unbound peptide monomer. For the fraction of peptide chains folded in the P_3M_3 complex (α_3), the fraction of peptide chains in the intermediate (α_i) and the fraction of unfolded monomers (β), equations 5 – 8 can be applied:

$$\alpha_3 = \frac{3[P_3M_3]}{P_0} \tag{5}$$

$$\alpha_i = \frac{\rho[P_\rho M_\mu]}{P_0} \tag{6}$$

$$\beta = \frac{[P]}{P_0} \tag{7}$$

$$\alpha_3 + \alpha_i + \beta = 1 \tag{8}$$

The concentration of free metal ions therefore becomes:

$$[M] = M_0 - 3[P_3M_3] - \mu[P_\rho M_\mu] \tag{9}$$

Rearranging eqs. (5-9) and substituting into eqs. (2) and (3) yields:

$$K_{Di} = \frac{\rho\left(P_0(1-\alpha_3-\alpha_i)\right)^\rho \left(M_0 - P_0\alpha_3 - \frac{\mu}{\rho}P_0\alpha_i\right)^\mu}{P_0\alpha_i} \tag{10}$$

$$K_{D3} = \frac{3\alpha_i\left(P_0(1-\alpha_3-\alpha_i)\right)^{3-\rho} \left(M_0 - P_0\alpha_3 - \frac{\mu}{\rho}P_0\alpha_i\right)^{3-\mu}}{\rho\alpha_3} \tag{11}$$

Peptide concentration [P_0] dependent titration data was fitted globally using a trust-region-reflective algorithm. During data fitting eqs. (10) and (11) are treated as a system of nonlinear equations with the two unknowns α_3 and α_i solved symbolically by the MATLAB function *solve(...)*. Numeric solutions for α_3 and α_i in the interval $0 < \alpha_3; \alpha_i < 1$ were calculated from the symbolic solutions using variable-precision arithmetic (MATLAB function *vpa(...)*) and the molar ellipticity [θ] was calculated using eqs. (8) and (4). The value of $[\theta]_f$ was set constant to the value of [θ] when no metal was added ($M_0 = 0$). pK_{D3} and pK_{Di} were left to vary freely and $[\theta]_{s3}$ and $[\theta]_{si}$ were left to vary in the interval $[\theta]_f \leq [\theta]_{s,3}$; $[\theta]_{s,i} \leq 40000$. The parameters pK_{D3}, pK_{Di}, $[\theta]_{s,3}$ and $[\theta]_{s,i}$ were shared parameters for all peptide concentrations during the global fit.

There are 9 possible intermediates when ρ=[1;2;3]; μ=[1;2;3], however ρ=3, μ=3 can be excluded from this list as this is the final oligomer state. Intermediate states where μ > ρ can also be excluded, leaving 5 possible intermediate states: P_1M_1, P_2M_1, P_2M_2, P_3M_1, and P_3M_2. All these intermediate states were fitted to the titration data using the method described above and the fits are shown in the figures below. The fitting parameters for the P_3M_1 intermediate, shown in the manuscript in Figure 4C & D, are given in Table S2 below for comparison.

Fitting parameters from the three-state model with a P_3M_1 intermediate

	HisAD:Cu(II)	HisAD:Ni(II)
$[\theta]_{si}$	-26.5 ± 4.5	-27.9 ± 2.5
$[\theta]_{s3}$	-19.5 ± 1.0	-23.5 ± 1.4
pK_{Di}	12.4 ± 0.5	13.5 ± 1.1
pK_{D3}	8.9 ± 0.9	9.9 ± 2.1

Table S2. Fit parameters with 95% confidence intervals for data fitted to the three-state model with a P_3M_1 intermediate; this intermediate gives the best fits. The fitted data is shown in the main manuscript, Fig. 4C-D.

Data and fits for alternative intermediates for the three-state fitting model

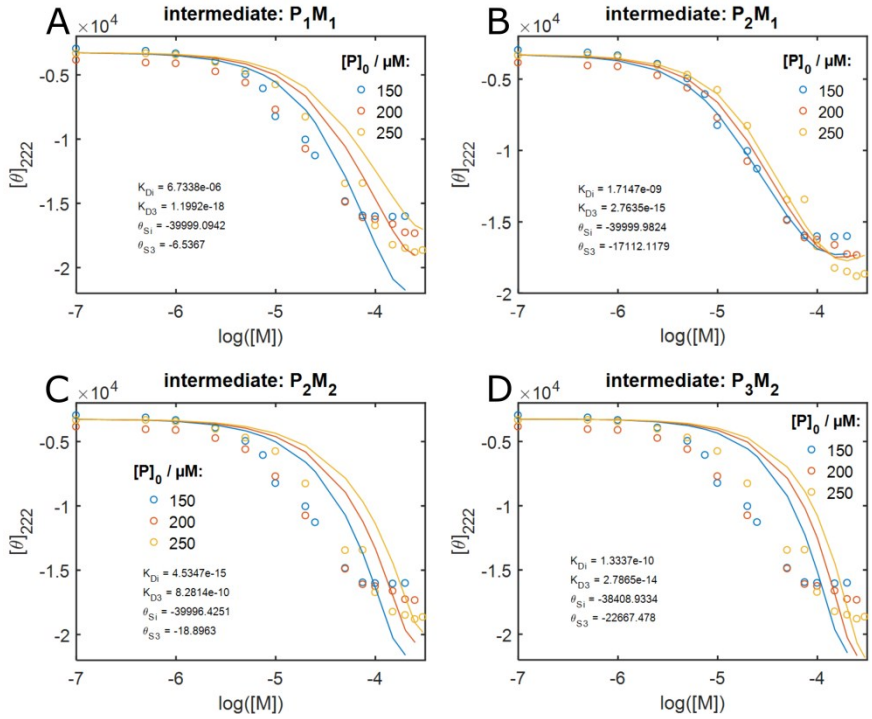

Figure S16. Titration curves for the HisAD:Cu(II) complex fitted to equations 10 and 11 assuming a (A) P_1M_1; (B) P_2M_1; (C) P_2M_2 and; (D) P_3M_2 intermediate. None of these intermediates resulted in good fits; the values for θ_{Si} were at the limit of fitting in each case.
Key: dots = experimental data; lines = fitted data.

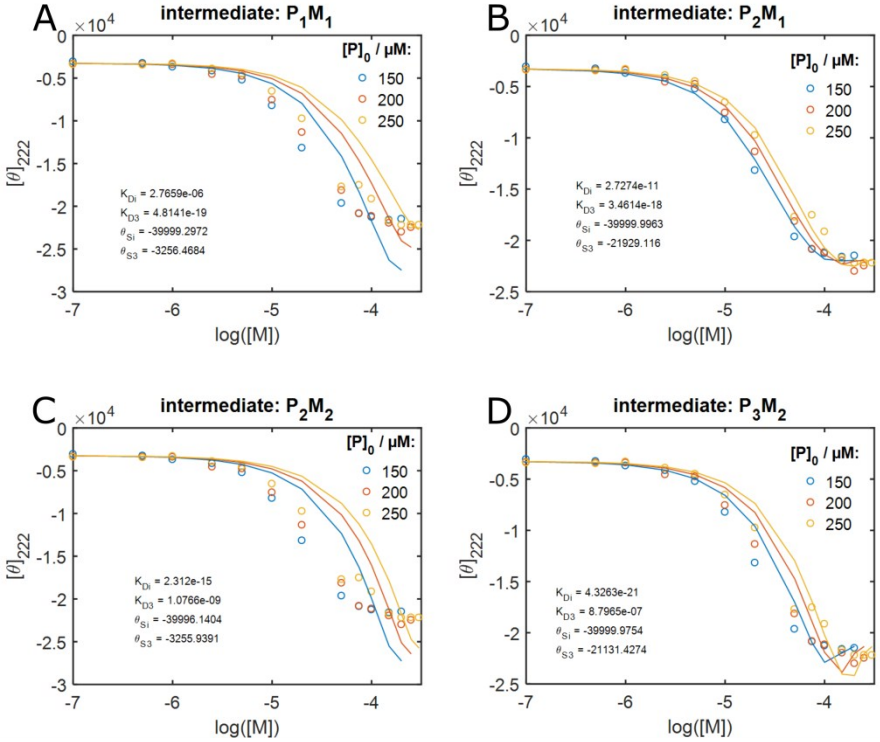

Figure S17. Titration curves for the HisAD:Ni(II) complex fitted to equations 10 and 11 assuming a (A) P_1M_1; (B) P_2M_1; (C) P_2M_2 and; (D) P_3M_2 intermediate. None of these intermediates resulted in good fits; the values for θ_{Si} were at the limit of fitting in each case.
Key: dots = experimental data; lines = fitted data.

LCMS spectra for HisA, HisD, HisAD, CC-Tri, and HisAD-WY

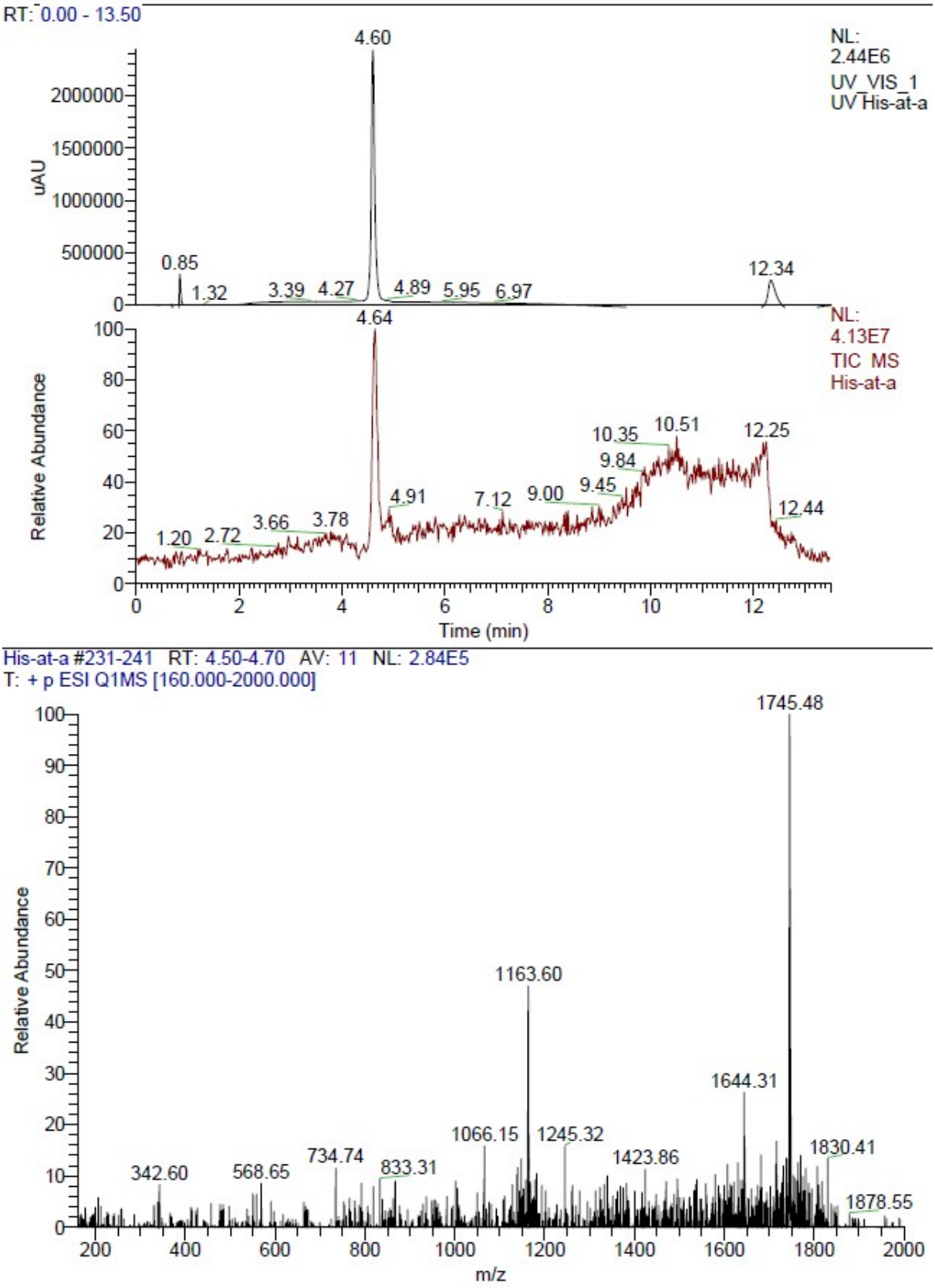

Figure S18. LCMS spectra for HisA.
Calculated mass: 3488.94 Da, observed masses: 1745.48 $[M + 2H^+]^{2+}$, 1163.60 $[M + 3H^+]^{3+}$

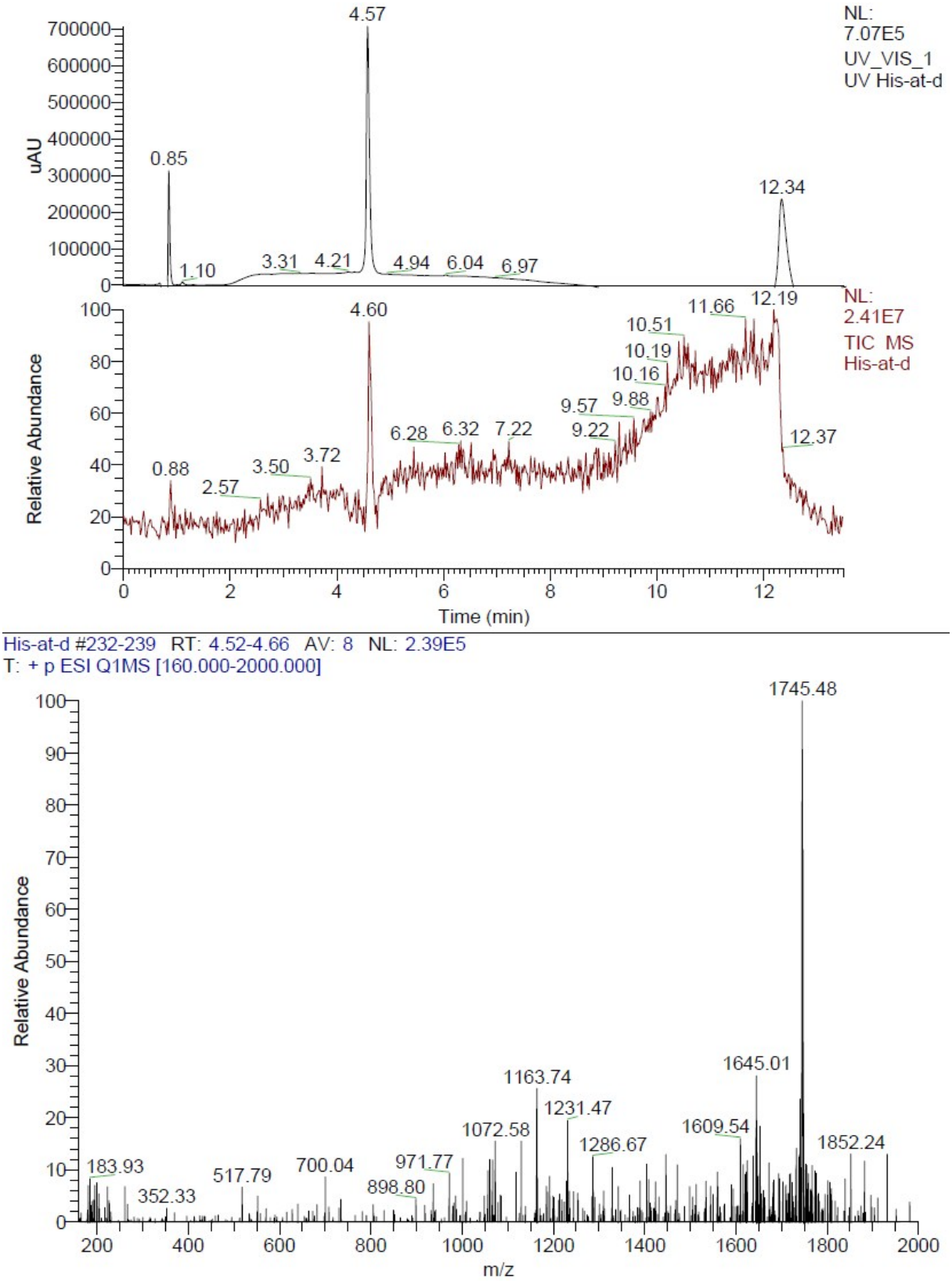

Figure S19. LCMS spectra for HisD.

Calculated mass: 3488.94 Da, observed mass: 1745.48 $[M + 2H^+]^{2+}$

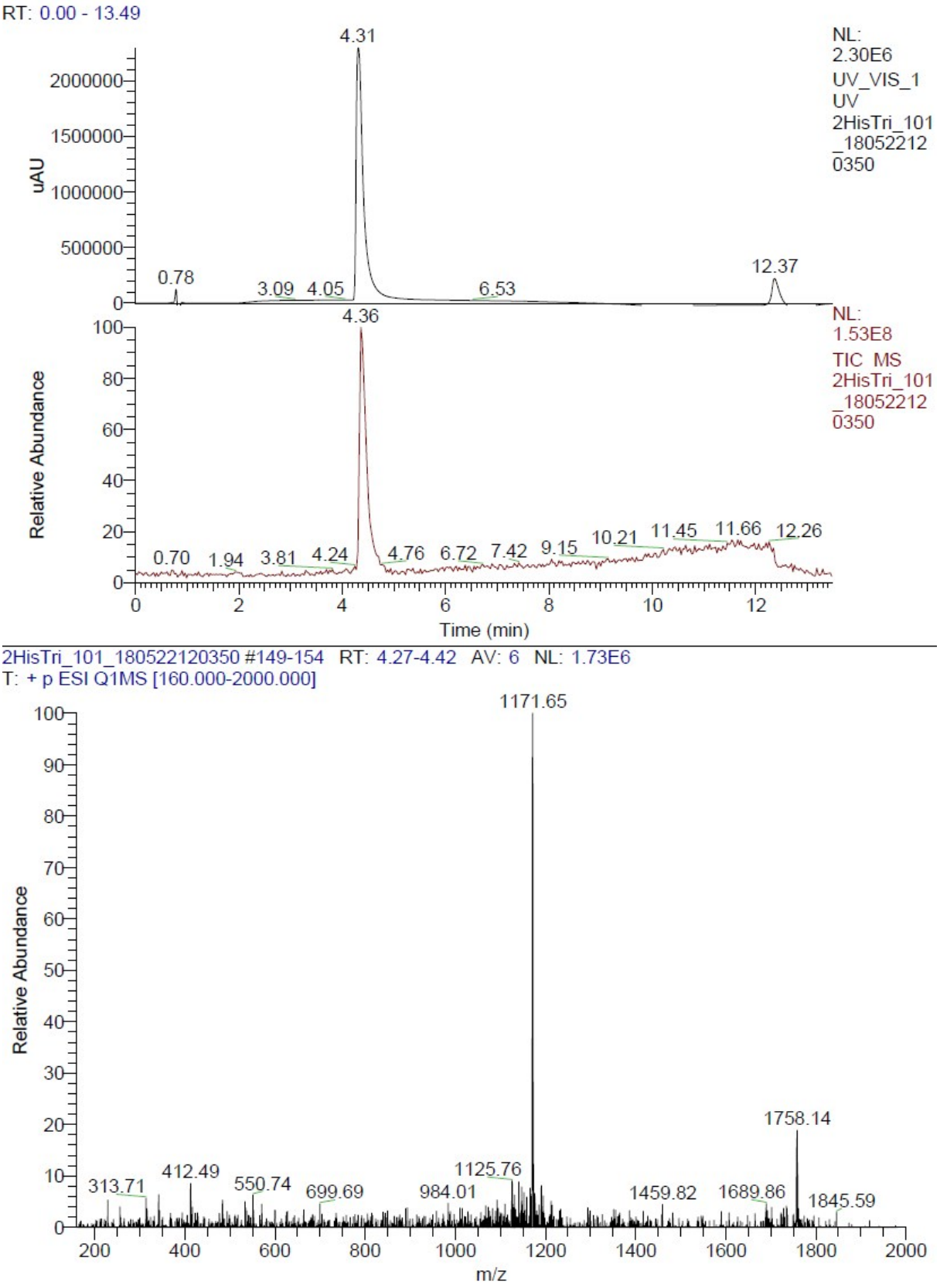

Figure S20. LCMS spectra for HisAD.

Calculated mass: 3512.92 Da, observed masses: 1758.14 $[M + 2H^+]^{2+}$, 1171.65 $[M + 3H^+]^{3+}$

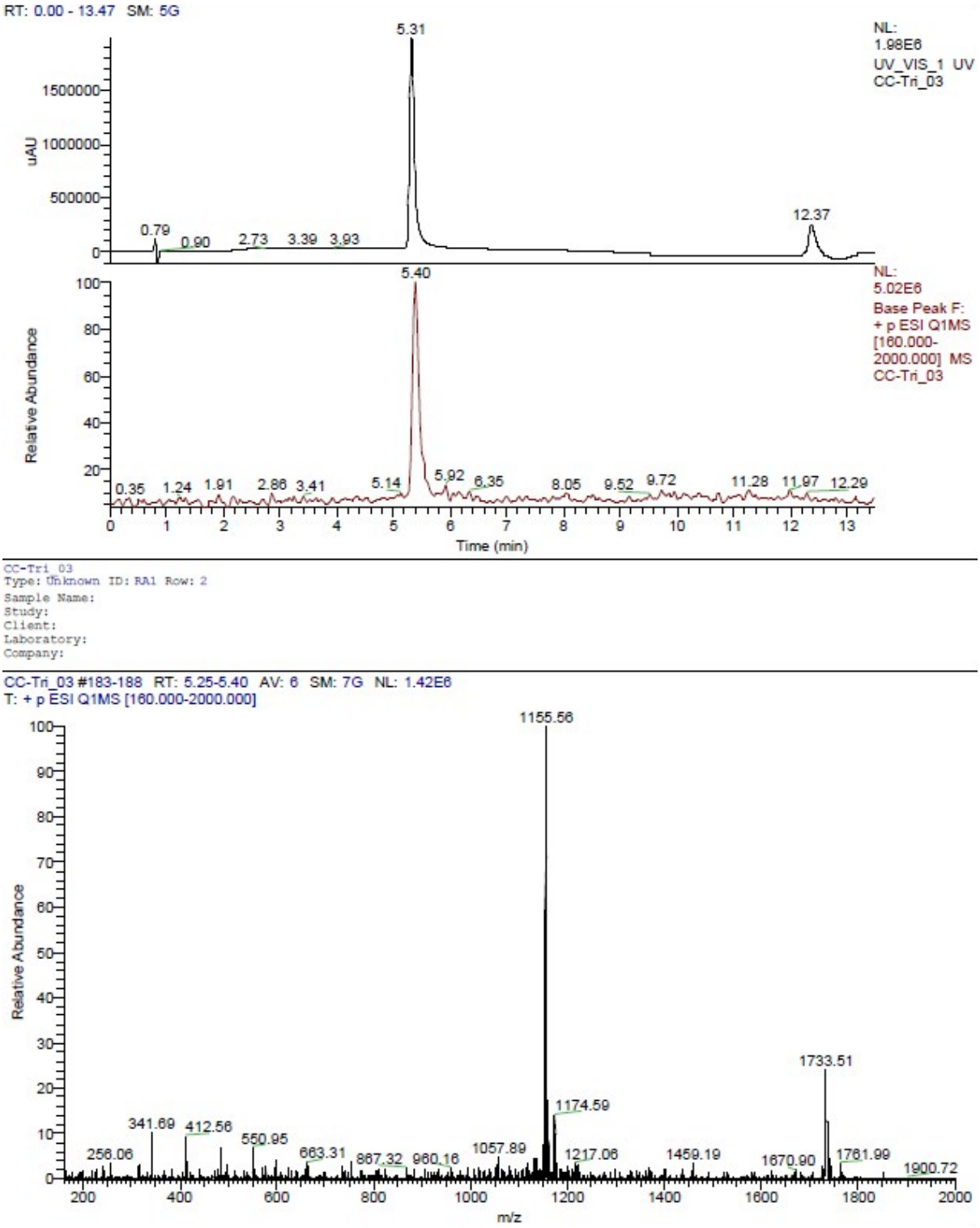

Figure S21. LCMS spectra for CC-Tri.

Calculated mass: 3465 Da, observed masses: 1733.51 $[M + 2H^+]^{2+}$, 1155.56 $[M + 3H^+]^{3+}$

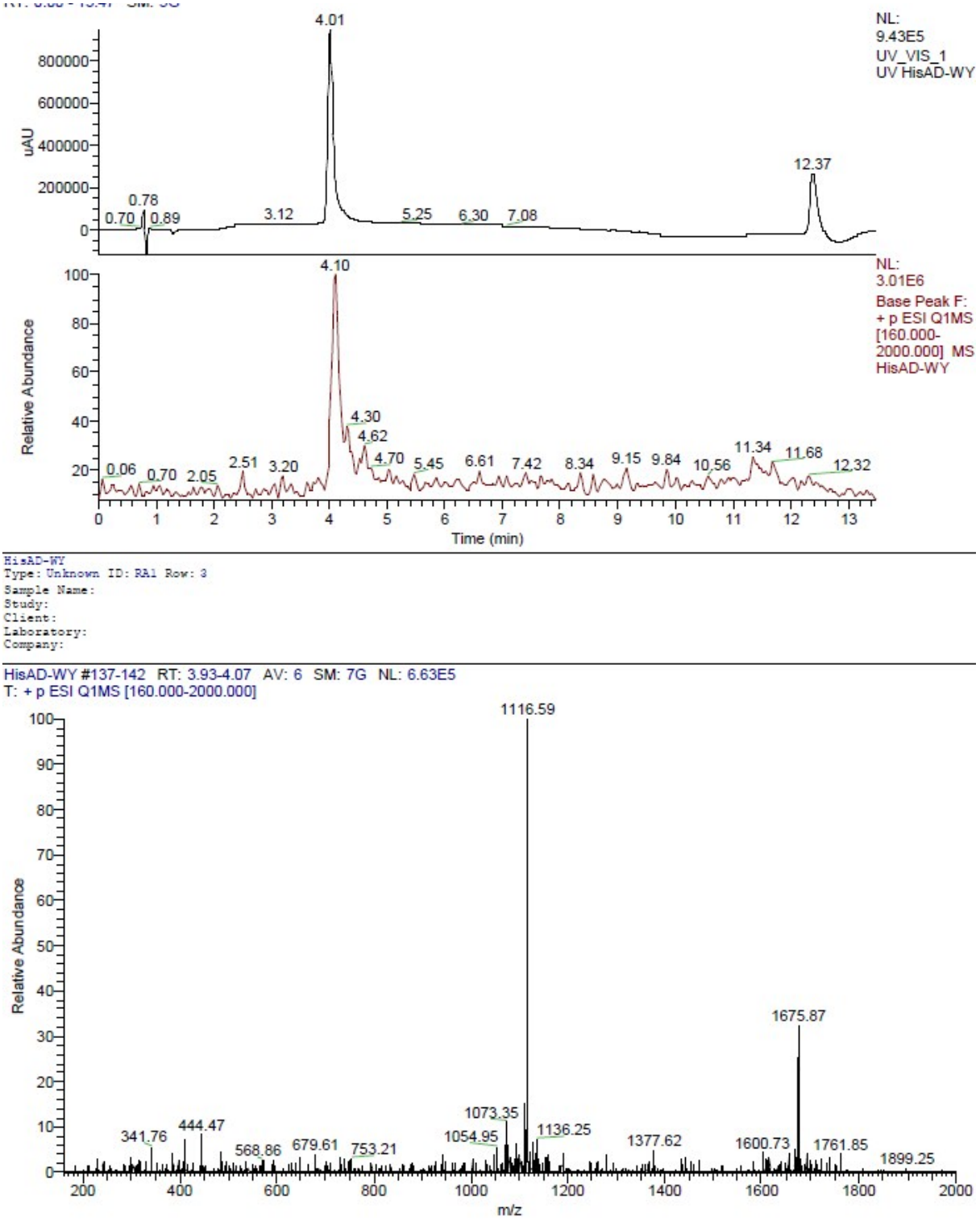

Figure S22. LCMS spectra for HisAD-WY.
Calculated mass: 3348.9 Da, observed masses: 1675.87 $[M + 2H^+]^{2+}$, 1116.59 $[M + 3H^+]^{3+}$